

1 **SUPPLEMENTARY INFORMATION**

2
3 **Gas-phase reactivity of CH₃OH toward OH at interstellar**
4 **temperatures (11.7-177.5 K): Experimental and theoretical**
5 **study**

6
7 Antonio J. Ocaña¹, Sergio Blázquez¹, Alexey Potapov², Bernabé Ballesteros^{1,3}, André
8 Canosa⁴, María Antiñolo³, Luc Vereecken^{5,*}, José Albaladejo^{1,3}, Elena Jiménez^{1,3,*}

- 9
10 1. *Departamento de Química Física. Facultad de Ciencias y Tecnologías Químicas.*
11 *Universidad de Castilla-La Mancha, Avda. Camilo José Cela, 1B. 13071 Ciudad*
12 *Real, Spain.*
13 1. *Laborastrophysikgruppe des Max-Planck-Instituts für Astronomie am Institut für*
14 *Festkörperphysik, Friedrich-Schiller-Universität Jena, Helmholtzweg 3, 07743*
15 *Jena, Germany.*
16 2. *Instituto de Investigación en Combustión y Contaminación Atmosférica (ICCA).*
17 *Universidad de Castilla-La Mancha, Avda. Moledores s/n. 13071 Ciudad Real,*
18 *Spain.*
19 3. *Département de Physique Moléculaire, Institut de Physique de Rennes, UMR*
20 *CNRS-UR1 6251, Université de Rennes 1, Campus de Beaulieu, 263 Avenue du*
21 *Général Leclerc, 35042 Rennes Cedex, France.*
22 4. *Forschungszentrum Juelich GmbH, IEK-8. Wilhelm-Johnen-Straße 52425 Jülich,*
23 *Germany.*

24

25 **Aerodynamic characterization of new Laval nozzles (He-15K and Ar-100K)**

26 The operational conditions of the He-15K and Ar-100 K nozzles are listed in Tables S1
 27 and S2 and the spatial profile of T is depicted in Figs. S1 and S2 for all conditions used with
 28 both nozzles. For the rest of the investigated temperatures the previously characterized Laval
 29 nozzles He-23K-LP (low pressure), He-23K-IP (intermediate pressure), He-23K-HP (high
 30 pressure), He-36 K and Ar-50K were used.^{1,2} When using the Ar-100K nozzle, the gas
 31 mixture was pulsed using the two-aperture rotatory disk (rotating at 5 Hz), as it was done for
 32 He-23K, He-36K and Ar-50K nozzles.¹ However, to achieve temperatures below 20 K (He-
 33 15K nozzle) with relatively low gas consumption and low pumping capacity, the disk with
 34 two apertures was replaced by a disk with one aperture of 16 mm×12 mm (length × height)
 35 dimensions which operates at 5 Hz.

36
 37 Table S1 Summary of the operating conditions employed for the pulsed He-15K Laval
 38 nozzle.^a

$P_{\text{res}} / \text{mbar}$	$P_{\text{cham}} / \text{mbar}$	M	$d_{\text{max}} / \text{cm}$	$t_{\text{hydro}} / \mu\text{s}$	$n / 10^{16} \text{ cm}^{-3}$	T / K
366.48	0.117	8.58	53	307	6.88 ± 0.62	11.7 ± 0.7
280.16	0.117	8.04	38	223	6.41 ± 0.55	13.0 ± 0.7
236.75	0.122	7.75	32	186	5.90 ± 0.52	14.3 ± 0.8
140.81	0.071	7.05	41	443	1.91 ± 0.25	22.1 ± 1.4

39 ^a Buffer gas is He (except for 22.1 K corresponding to a mixture of 50% N₂ and 50% He) and the
 40 temperature of the reservoir was constant ($T_{\text{res}} = 297 \pm 2 \text{ K}$); Uncertainties in n and T are $\pm 1\sigma$ (standard
 41 deviation) and represent the fluctuations of physical parameters along the length of uniformity of the
 42 flow.

Table S2 Summary of the operating conditions employed for the pulsed Ar-100K Laval nozzle. ^a

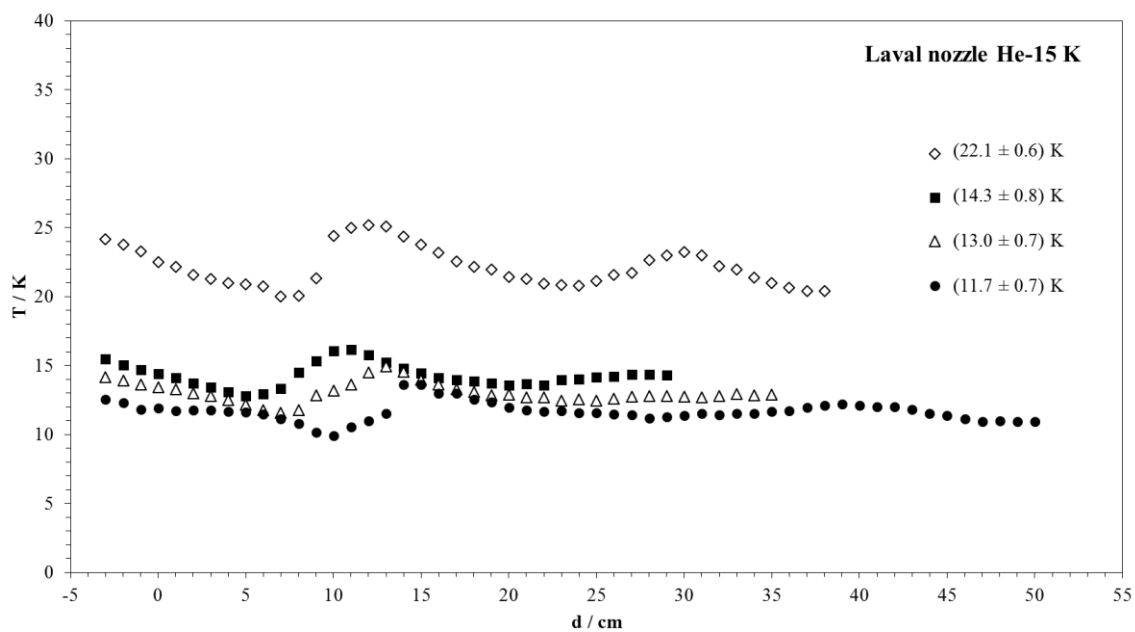
Buffer Gas	$P_{\text{res}}/\text{mbar}$	$P_{\text{cham}}/\text{mbar}$	M	d_{max}/cm	$t_{\text{hydro}}/\mu\text{s}$	$n / 10^{16} \text{ cm}^{-3}$	T/K
Ar	109.73	5.960	2.65	18	387	43.38 ± 0.51	89.1 ± 0.7
	37.66	3.053	2.39	29	646	18.34 ± 0.17	101.8 ± 0.6
	27.09	2.515	2.32	28	630	14.02 ± 0.11	106.0 ± 0.6
	16.16	1.964	2.16	27	625	9.58 ± 0.14	115.3 ± 1.1
	11.28	1.600	2.07	15	352	7.20 ± 0.08	122.5 ± 1.0
N ₂	71.99	5.200	2.43	16	277	24.92 ± 0.35	136.1 ± 0.8
	57.94	4.707	2.36	20	351	21.68 ± 0.40	140.4 ± 1.0
	43.77	3.822	2.32	22	389	17.02 ± 0.17	143.3 ± 0.6
	29.10	2.923	2.24	27	485	12.35 ± 0.13	148.3 ± 0.6
	24.25	2.607	2.21	25	453	10.69 ± 0.12	149.9 ± 0.7
	19.42	2.281	2.15	23	424	9.14 ± 0.11	153.1 ± 0.7
	14.37	1.961	2.07	17	320	7.40 ± 0.07	158.8 ± 0.6
	9.96	1.566	1.98	10	192	5.64 ± 0.08	165.7 ± 0.9
	9.97	2.000	1.83	9	181	6.71 ± 0.11	177.5 ± 1.2

^a The temperature of the reservoir was constant ($T_{\text{res}} = 297 \pm 2 \text{ K}$); Uncertainties in n and T are $\pm 1\sigma$ (standard deviation) and represent the fluctuations of physical parameters along the length of uniformity of the flow.

49

50

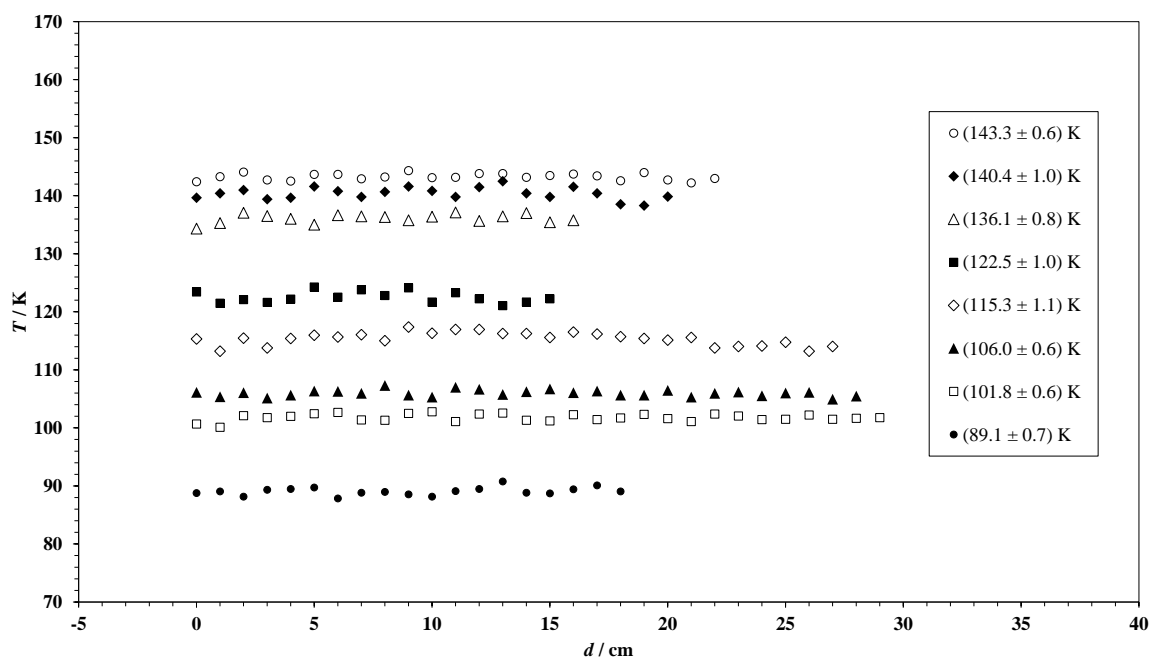
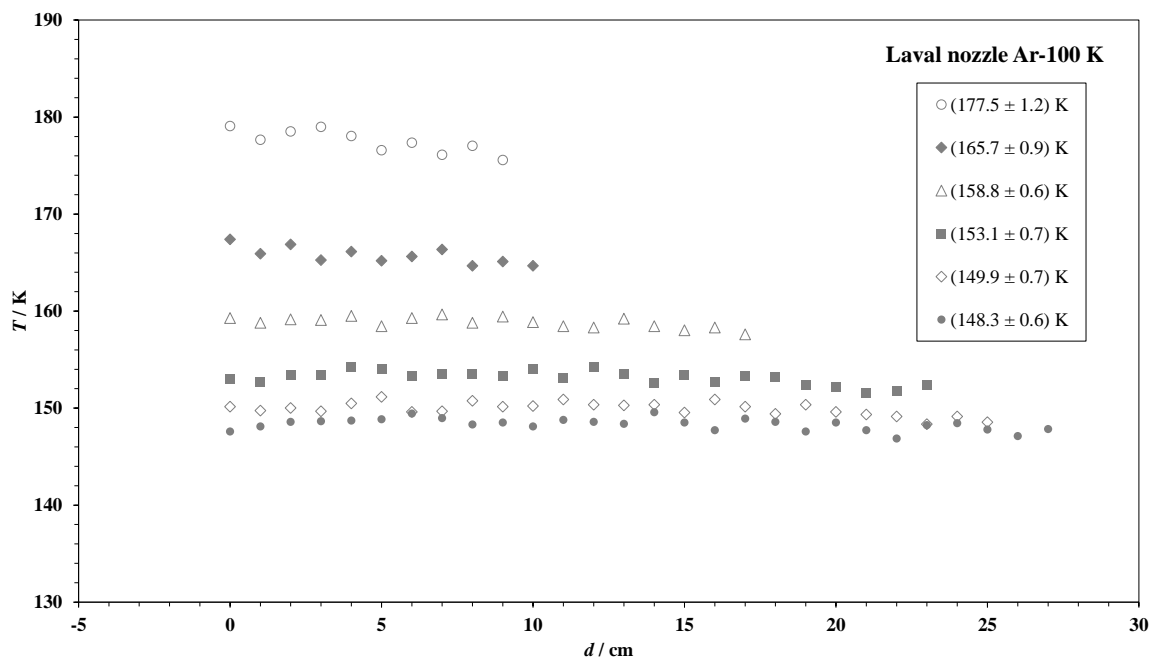
51



52

53 **Fig. S1** Spatial profiles of the jet temperature obtained with the Laval nozzle He-15K.

54



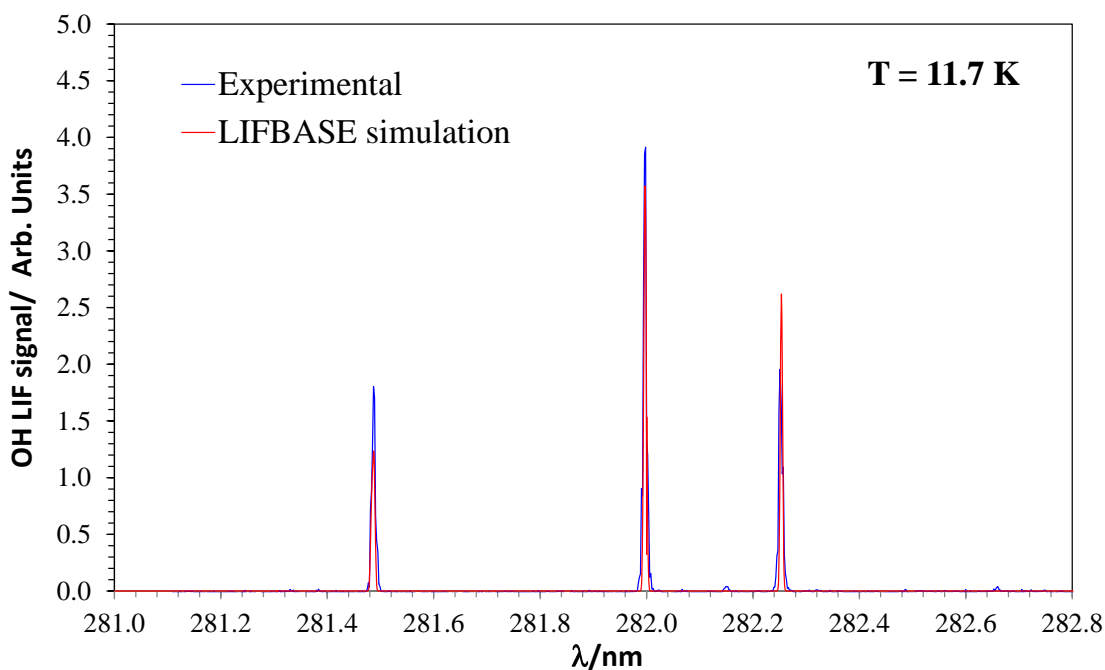
55

56 **Fig. S2** Spatial profiles of the jet temperature obtained with the Laval nozzle Ar-100K.

57

58

59 Additionally to the Pitot measurements, the conventional pulsed laser photolysis-laser
60 induced fluorescence (PLP-LIF) technique was used for recording the “ultra-cold” LIF
61 spectrum of OH radicals between 281.0 and 282.8 nm with a spectral resolution of 0.002 nm
62 or 0.004 nm at a fixed reaction time (40 μ s). OH radicals were generated *in situ* in the jet by
63 laser photolysis at 248 nm of a molecular precursor (H_2O_2 or tertbutyl hydroperoxide (t-
64 BuOOH, $(CH_3)_3COOH$)). The LIF signal from OH radicals was monitored at ca. 309 nm,
65 after laser excitation of electronic ground state OH at 282 nm. In Fig. S3, the recorded LIF
66 spectrum at 11.7 K is shown together with the simulated one using LIFBASE software
67 version 2.1 assuming thermalization of the system.³
68



69
70 **Fig. S3** Examples of the LIF spectrum of OH radicals recorded in the absence of
71 methanol at 11.7 K and 40 μ s delay time between the photolysis and the excitation lasers.

72

73

74 **Determination of the methanol concentration by UV spectroscopy at 185 nm**

75 Mixtures of gaseous methanol and a buffer gas (He, Ar or N₂) were prepared in a 50-L
76 storage bulb. The dilution factor, f , in the bulb was calculated as $P_{\text{methanol}}/(P_{\text{methanol}}+P_{\text{buffer}})$ and
77 ranged from 1.7×10^{-3} to 0.1. Typically, f was 1×10^{-2} (see Table S3). To check these values
78 directly related to methanol concentration, UV spectroscopy at 185 nm was employed.

79 Introducing a known total pressure (P_{Total}) from the bulb in a 107-cm absorption cell, the
80 absorbance ($A_{\lambda=185\text{nm}}$) was measured as $\ln(I_0/I)$. The transmitted intensities at 185 nm from a
81 Hg/Ar-pen ray in the absence and presence of methanol (I_0 and I , respectively) were detected
82 in a filtered phototube. From the slope of the plots of the absorbance $A_{\lambda=185\text{nm}}$ versus P_{Total} ,
83 the dilution factor of methanol in the bulb was obtained:

84
$$A_{\lambda=185\text{nm}} = \frac{\sigma_{\lambda=185\text{nm}} \times l \times f}{RT} \times P_{\text{Total}} \quad (\text{E.I})$$

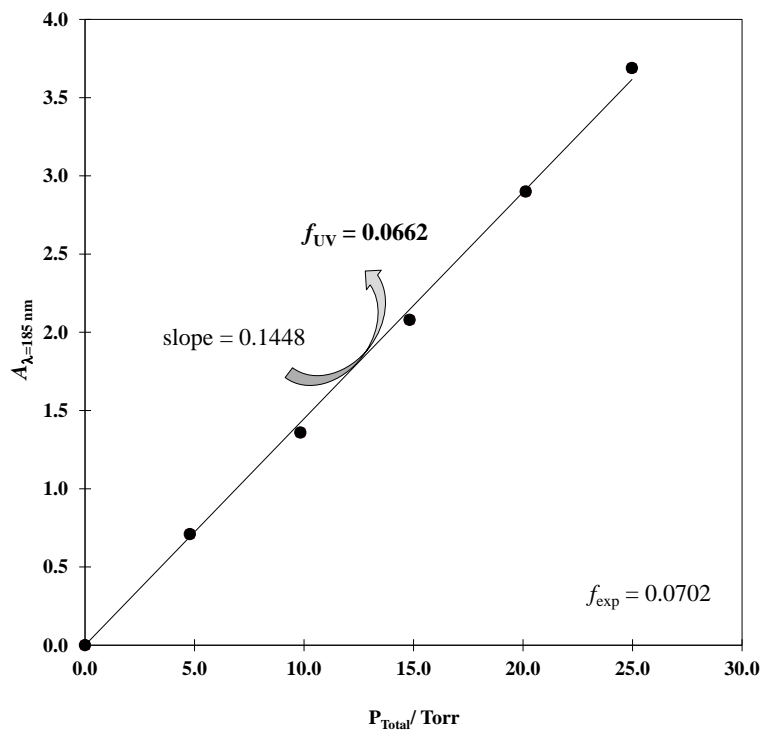
85 using the absorption cross section (in base e), $\sigma_{\lambda=185\text{nm}} = 6.3 \times 10^{-19} \text{ cm}^2 \text{ molecule}^{-1}$, reported
86 at 185 nm by Jiménez et al.⁴. An example of the plots of eqn (E.I) is presented in Fig. S4.
87 The good linearity implies that the Beer-Lambert law is valid in the concentration range in
88 the absorption cell ($(1-6) \times 10^{16} \text{ cm}^{-3}$).

89

90

91 **References**

- 92 1 E. Jiménez, B. Ballesteros, A. Canosa, T. M. Townsend, F. J. Maigler, V. Napal, B.
93 R. Rowe and J. Albaladejo, Development of a pulsed uniform supersonic gas
94 expansion system based on an aerodynamic chopper for gas phase reaction kinetic
95 studies at ultra-low temperatures, *Rev. Sci. Instrum.*, 2015, **86**, 45108.
- 96 2 A. Canosa, A. J. Ocaña, M. Antiñolo, B. Ballesteros, E. Jiménez and J. Albaladejo,
97 Design and testing of temperature tunable de Laval nozzles for applications in gas-
98 phase reaction kinetics, *Exp. Fluids*, 2016, **57**, 1–14.
- 99 3 D. R. Luque, J. and Crosley, LIFBASE version 2.1 (SRI International, Menlo Park,
100 CA, 1999), available at www.sri.com/psd/lifbase
- 101 4 E. Jiménez, M. K. Gilles and A. R. Ravishankara, Kinetics of the reactions of the
102 hydroxyl radical with CH₃OH and C₂H₅OH between 235 and 360 K, *J. Photochem.*
103 *Photobiol. A Chem.*, 2003, **157**, 237–245.
- 104 5 S. Xu and M. C. Lin, Theoretical study on the kinetics for OH reactions with CH₃OH
105 and C₂H₅OH, *Proc. Combust. Inst.*, 2007, **31**, 159–166.
- 106 6 L. G. Gao, J. Zheng, A. Fernández-Ramos, D. G. Truhlar and X. Xu, Kinetics of the
107 Methanol Reaction with OH at Interstellar, Atmospheric, and Combustion
108 Temperatures, *J. Am. Chem. Soc.*, 2018, **140**, 2906–2918.
- 109 7 O. Roncero, A. Zanchet and A. Aguado, Low temperature reaction dynamics for
110 CH₃OH + OH collisions on a new full dimensional potential energy surface, *Phys.*
111 *Chem. Chem. Phys.*, 2018, **20**, 25951–25958.
- 112 8 W. Siebrand, Z. Smedarchina, E. Martínez-Núñez and A. Fernández-Ramos,
113 Methanol dimer formation drastically enhances hydrogen abstraction from methanol
114 by OH at low temperature, *Phys. Chem. Chem. Phys.*, 2016, **18**, 22712–22718.
- 115
- 116
- 117
- 118
- 119



120

121 **Fig. S4.** Example of the measurement of the absorbance at 185 nm as a function of
 122 total pressure from a bulb with diluted methanol to check the dilution factor.

123

124

125

126

127
128
129

Table S3 Summary of the experimental conditions employed in the kinetic study: methanol dilution factor (f), mass flow rates (F in liters or cubic centimeters per minute – slpm or sccm- in standard conditions) and the range of methanol concentration used in the kinetic analysis.

T/ K	$f \times 10^{-3}$	$F_{\text{Buffer}}/$ slpm*	$F_{\text{OH-precursor}}/$ sccm	$F_{\text{methanol/buffer}}/$ sccm	$[\text{CH}_3\text{OH}]/$ 10^{14} cm^{-3}	% CH_3OH in the jet
11.7 ± 0.7	5	5.05	100 ^a	80.8 – 423.3	0.05 – 0.28	0.008 – 0.041
13.0 ± 0.7	4 – 14	3.84	100 ^a	80.3 – 718.1	0.06 – 0.40	0.010 – 0.060
14.3 ± 0.8	4	3.14	100 ^a	80.9 – 620.0	0.03 – 0.25	0.005 – 0.042
21.1 ± 0.6	6 – 54	5.80	20 ^a	50.3 – 715.9	0.09 – 0.63	0.035 – 0.188
21.7 ± 1.4	6 – 30	9.33	30 – 100 ^a	51.1 – 374.0	0.08 – 0.54	0.005 – 0.033
22.1 ± 1.4	8	2.58	50 ^a	80.6 – 373.1	0.09 – 0.41	0.047 – 0.213
22.5 ± 0.7	17 – 21	10.1	30 ^a	51.1 – 369.0	0.08 – 0.49	0.011 – 0.066
36.2 ± 1.2	5 – 8	12.6	70 ^a	101.4 – 557.7	0.06 – 0.51	0.003 – 0.029
45.3 ± 1.3	5 – 8	1.38	20 ^a	53.0 – 517.6	0.10 – 1.28	0.023 – 0.302
49.9 ± 1.4	5 – 10	3.91	20 ^a	71.1 – 694.6	0.08 – 1.45	0.009 – 0.174
50.5 ± 1.6	9 – 50	1.28	20 ^a	66.4 – 516.2	0.08 – 2.75	0.051 – 2.029
51.6 ± 1.7	13 – 73	12.8	50 – 200 ^a	64.7 – 1435.6	0.08 – 1.15	0.020 – 0.275
52.1 ± 0.5	5 – 15	4.63	20 – 30 ^a	30.3 – 121.1	0.09 – 0.44	0.005 – 0.023
64.1 ± 1.6	4 – 8	1.86	20 – 30 ^a	50.4 – 523.6	0.09 – 0.95	0.020 – 0.205
68.8 ± 0.6	13	5.04	20 ^a	31.0 – 123.6	0.14 – 0.54	0.008 – 0.033
69.5 ± 1.6	4 – 8	1.33	20 ^a	49.7 – 514.9	0.09 – 1.01	0.029 – 0.310
89.1 ± 0.7	6	7.79	50 ^b	49.9 – 220.2	0.15 – 0.66	0.003 – 0.015
89.5 ± 0.6	4	7.57	21 ^a	96.3 – 514.9	0.10 – 0.53	0.010 – 0.030

99.3 ± 0.4	4 – 8	2.46	12 ^a	49.7 – 467.4	0.07 – 1.17	0.010 – 0.150
101.8 ± 0.6	6	2.46	10 ^a	49.9 – 348.0	0.16 – 1.15	0.012 – 0.082
106.0 ± 0.6	5	1.73	5 ^a	50.7 – 557.8	0.21 – 2.29	0.015 – 0.163
107.0 ± 0.5	6 – 17	1.27	5 – 10 ^a	31.2 – 381.1	0.12 – 2.80	0.030 – 0.570
115.3 ± 1.1	8	0.96	2 ^a	49.8 – 432.1	0.39 – 3.07	0.041 – 0.321
122.5 ± 1.0	2– 15	0.63	4 ^{a, b}	49.4 – 302.0	0.84 – 5.11	0.117 – 0.709
136.1 ± 0.8	23	5.64	2 ^{a, b}	49.2 – 509.1	0.50 – 5.16	0.020 – 0.207
140.4 ± 1.0	55	4.43	10 ^{a, b}	48.3 – 499.3	1.32 – 13.6	0.061 – 0.625
143.3 ± 0.6	10	3.35	20 ^a	49.6 – 513.2	0.26 – 2.60	0.015 – 0.153
148.3 ± 0.6	30	2.19	4 ^b	48.6 – 378.8	0.83 – 6.41	0.067 – 0.519
149.9 ± 0.7	24	1.81	1 ^{a, b}	48.7 – 131.6	0.71 – 1.90	0.066 – 0.177
153.1 ± 0.7	30	1.42	2 ^{a, b}	48.6 – 420.1	0.94 – 8.04	0.103 – 0.880
158.8 ± 0.6	24	1.02	0.4 ^{a, b}	48.7 – 463.0	0.86 – 8.12	0.116 – 1.096
165.7 ± 0.9	50 – 100	0.67	0.4 – 1 ^{a, b}	46.8 – 251.9	2.00 – 11.1	0.354 – 1.972
177.5 ± 1.2	50 – 100	0.65	0.4 – 1 ^{a, b}	46.8 – 455.8	2.43 – 39.3	0.363 – 5.864

* In each kinetic experiment, the main flow (F_{Buffer}) was slightly changed when varying the methanol flow rate ($F_{\text{methanol/buffer}}$) in order to keep the $F_{\text{OH-precursor}}/F_{\text{Total}}$ ratio constant and, therefore, [OH-precursor] and k_0 constants; ^a H₂O₂; ^b *t*-BuOOH

130
131

132
133
134

Table S4 Predicted high-pressure rate coefficients ($\text{cm}^3 \text{ molecule}^{-1} \text{ s}^{-1}$ for k_a and k_{HPL} ; s^{-1} for k_{-a} , k_{b1} and k_{b2}) and product yields for the reaction steps in the $\text{CH}_3\text{OH} + \text{OH}$ mechanism. $k_{b1}(\text{T})$ and $k_{b2}(\text{T})$ HPL predictions below 50K are considered unreliable (see main text) and are not reported.

T / K	$k_a(\text{T})$	$k_{-a}(\text{T})$	$k_{b1}(\text{T})$	$k_{b2}(\text{T})$	$k_{\text{HPL}}(\text{T})$	Yield CH_2OH	Yield CH_3O
20	4.23×10^{-11}	1.92×10^{-40}			4.23×10^{-11}		
30	4.31×10^{-11}	1.02×10^{-22}			4.31×10^{-11}		
40	4.11×10^{-11}	8.22×10^{-14}			4.11×10^{-11}		
50	3.89×10^{-11}	1.90×10^{-8}	8.57×10^{-2}	5.74	3.89×10^{-11}	0.015	0.985
60	3.70×10^{-11}	7.31×10^{-5}	3.01×10^{-1}	16.5	3.70×10^{-11}	0.018	0.982
70	3.56×10^{-11}	2.69×10^{-2}	1.16	46.2	3.56×10^{-11}	0.025	0.975
80	3.45×10^{-11}	2.27	5.09	1.23×10^2	3.43×10^{-11}	0.040	0.960
90	3.37×10^{-11}	7.20×10	23.6	3.08×10^2	3.14×10^{-11}	0.071	0.929
100	3.32×10^{-11}	1.15×10^3	1.07×10^2	7.17×10^2	2.26×10^{-11}	0.130	0.870
110	3.28×10^{-11}	1.10×10^4	4.48×10^2	1.57×10^3	1.15×10^{-11}	0.222	0.778
120	3.25×10^{-11}	7.28×10^4	1.70×10^3	3.25×10^3	5.46×10^{-12}	0.343	0.657
130	3.23×10^{-11}	3.59×10^5	5.76×10^3	6.42×10^3	2.96×10^{-12}	0.473	0.527
140	3.22×10^{-11}	1.41×10^6	1.76×10^4	1.22×10^4	1.90×10^{-12}	0.591	0.409
150	3.22×10^{-11}	4.61×10^6	4.84×10^4	2.22×10^4	1.41×10^{-12}	0.685	0.315
160	3.22×10^{-11}	1.30×10^7	1.22×10^5	3.93×10^4	1.15×10^{-12}	0.756	0.244
170	3.23×10^{-11}	3.23×10^7	2.82×10^5	6.74×10^4	1.01×10^{-12}	0.807	0.193
180	3.23×10^{-11}	7.25×10^7	6.08×10^5	1.13×10^5	9.30×10^{-13}	0.844	0.156
190	3.25×10^{-11}	1.49×10^8	1.23×10^6	1.84×10^5	8.88×10^{-13}	0.870	0.130
200	3.26×10^{-11}	2.85×10^8	2.34×10^6	2.92×10^5	8.70×10^{-13}	0.889	0.111
210	3.28×10^{-11}	5.12×10^8	4.23×10^6	4.55×10^5	8.68×10^{-13}	0.903	0.097
220	3.29×10^{-11}	8.69×10^8	7.31×10^6	6.93×10^5	8.77×10^{-13}	0.913	0.087
230	3.31×10^{-11}	1.41×10^9	1.21×10^7	1.03×10^6	8.95×10^{-13}	0.921	0.079
240	3.33×10^{-11}	2.18×10^9	1.94×10^7	1.52×10^6	9.21×10^{-13}	0.928	0.072
250	3.34×10^{-11}	3.27×10^9	3.01×10^7	2.18×10^6	9.52×10^{-13}	0.932	0.068
260	3.36×10^{-11}	4.73×10^9	4.53×10^7	3.08×10^6	9.89×10^{-13}	0.936	0.064

270	3.38×10^{-11}	6.65×10^9	6.63×10^7	4.28×10^6	1.03×10^{-12}	0.939	0.061
280	3.40×10^{-11}	9.11×10^9	9.48×10^7	5.86×10^6	1.08×10^{-12}	0.942	0.058
290	3.42×10^{-11}	1.22×10^{10}	1.32×10^8	7.91×10^6	1.12×10^{-12}	0.944	0.056
300	3.43×10^{-11}	1.60×10^{10}	1.82×10^8	1.05×10^7	1.18×10^{-12}	0.945	0.055
310	3.45×10^{-11}	2.05×10^{10}	2.44×10^8	1.38×10^7	1.23×10^{-12}	0.947	0.053
320	3.46×10^{-11}	2.59×10^{10}	3.23×10^8	1.79×10^7	1.29×10^{-12}	0.947	0.053
330	3.48×10^{-11}	3.22×10^{10}	4.21×10^8	2.30×10^7	1.36×10^{-12}	0.948	0.052
340	3.49×10^{-11}	3.95×10^{10}	5.41×10^8	2.91×10^7	1.42×10^{-12}	0.949	0.051
350	3.51×10^{-11}	4.78×10^{10}	6.87×10^8	3.66×10^7	1.49×10^{-12}	0.949	0.051
360	3.52×10^{-11}	5.71×10^{10}	8.60×10^8	4.55×10^7	1.57×10^{-12}	0.950	0.050
370	3.53×10^{-11}	6.75×10^{10}	1.07×10^9	5.60×10^7	1.64×10^{-12}	0.950	0.050
380	3.54×10^{-11}	7.90×10^{10}	1.31×10^9	6.84×10^7	1.72×10^{-12}	0.950	0.050
390	3.55×10^{-11}	9.15×10^{10}	1.59×10^9	8.28×10^7	1.80×10^{-12}	0.950	0.050

135

136

137
138
139

Table S5 Predicted low-pressure limit rate coefficient ($k_{\text{LPL}}(T)$ in $\text{cm}^3 \text{ molecule}^{-1} \text{ s}^{-1}$) and product yields for the reaction steps in the $\text{CH}_3\text{OH} + \text{OH}$ mechanism.

T / K	$k_{\text{LPL}}(T)$	CH_2OH Yield	CH_3O Yield
20	2.29×10^{-11}	0.711	0.289
30	1.47×10^{-11}	0.712	0.288
40	9.35×10^{-12}	0.713	0.287
50	6.19×10^{-12}	0.714	0.286
60	4.30×10^{-12}	0.715	0.285
70	3.13×10^{-12}	0.716	0.284
80	2.37×10^{-12}	0.717	0.283
90	1.86×10^{-12}	0.718	0.282
100	1.50×10^{-12}	0.719	0.281
110	1.25×10^{-12}	0.721	0.279
120	1.06×10^{-12}	0.723	0.277
130	9.15×10^{-13}	0.725	0.275
140	8.08×10^{-13}	0.727	0.273
150	7.26×10^{-13}	0.730	0.270
160	6.63×10^{-13}	0.733	0.267
170	6.14×10^{-13}	0.736	0.264
180	5.77×10^{-13}	0.740	0.260
190	5.48×10^{-13}	0.744	0.256
200	5.27×10^{-13}	0.748	0.252
210	5.13×10^{-13}	0.752	0.248
220	5.03×10^{-13}	0.757	0.243
230	4.98×10^{-13}	0.762	0.238
240	4.96×10^{-13}	0.767	0.233
250	4.98×10^{-13}	0.772	0.228
260	5.03×10^{-13}	0.776	0.224
270	5.11×10^{-13}	0.781	0.219
280	5.21×10^{-13}	0.786	0.214
290	5.34×10^{-13}	0.791	0.209
300	5.49×10^{-13}	0.795	0.205
310	5.66×10^{-13}	0.800	0.200
320	5.85×10^{-13}	0.804	0.196
330	6.06×10^{-13}	0.808	0.192
340	6.29×10^{-13}	0.812	0.188
350	6.53×10^{-13}	0.815	0.185
360	6.79×10^{-13}	0.819	0.181
370	7.07×10^{-13}	0.822	0.178
380	7.37×10^{-13}	0.825	0.175
390	7.68×10^{-13}	0.828	0.172

140

141 Table S6 Predicted high- and low-pressure rate coefficients ($\text{cm}^3 \text{ molecule}^{-1} \text{ s}^{-1}$ for k_a and k_{HPL} ; s^{-1} for k_{-a} , k_{b1} and k_{b2}) and product yields
 142 for the reaction steps in the $\text{CH}_3\text{OH} + \text{OH}$ mechanism, after adjustment of the barrier heights for H-abstraction to match the IUPAC
 143 $k(300\text{K})$ and the CH_3O yield recommendations, and scaling the low-energy capture rate coefficient to the average of the experimental
 144 $k(20\text{K})$ values. CH_2OH and CH_3O HPL yields below 50K are considered unreliable (see main text) and are not reported.

T / K	$k_{\text{capture}}(\text{T})$	$k_{\text{HPL}}(\text{T})$	CH_2OH Yield HPL	CH_3O Yield HPL	$k_{\text{LPL}}(\text{T})$	CH_2OH Yield LPL	CH_3O Yield LPL
20	6.79×10^{-11}	6.79×10^{-11}			3.39×10^{-11}	0.503	0.497
30	6.46×10^{-11}	6.46×10^{-11}			2.18×10^{-11}	0.505	0.495
40	5.68×10^{-11}	5.68×10^{-11}			1.35×10^{-11}	0.508	0.492
50	4.96×10^{-11}	4.96×10^{-11}	0.000	1.000	8.55×10^{-12}	0.511	0.489
60	4.42×10^{-11}	4.42×10^{-11}	0.000	1.000	5.64×10^{-12}	0.513	0.487
70	4.04×10^{-11}	4.04×10^{-11}	0.000	1.000	3.93×10^{-12}	0.516	0.484
80	3.78×10^{-11}	3.78×10^{-11}	0.001	0.999	2.87×10^{-12}	0.519	0.481
90	3.60×10^{-11}	3.58×10^{-11}	0.002	0.998	2.18×10^{-12}	0.523	0.477
100	3.48×10^{-11}	3.29×10^{-11}	0.005	0.995	1.72×10^{-12}	0.526	0.474
110	3.39×10^{-11}	2.60×10^{-11}	0.014	0.986	1.40×10^{-12}	0.531	0.469
120	3.34×10^{-11}	1.57×10^{-11}	0.031	0.969	1.17×10^{-12}	0.535	0.465
130	3.30×10^{-11}	8.03×10^{-12}	0.065	0.935	1.00×10^{-12}	0.540	0.460
140	3.27×10^{-11}	4.17×10^{-12}	0.118	0.882	8.75×10^{-13}	0.546	0.454
150	3.26×10^{-11}	2.42×10^{-12}	0.191	0.809	7.78×10^{-13}	0.552	0.448
160	3.25×10^{-11}	1.59×10^{-12}	0.279	0.721	7.04×10^{-13}	0.559	0.441
170	3.25×10^{-11}	1.18×10^{-12}	0.371	0.629	6.46×10^{-13}	0.566	0.434
180	3.25×10^{-11}	9.53×10^{-13}	0.459	0.541	6.02×10^{-13}	0.574	0.426
190	3.26×10^{-11}	8.30×10^{-13}	0.536	0.464	5.68×10^{-13}	0.582	0.418
200	3.27×10^{-11}	7.62×10^{-13}	0.602	0.398	5.43×10^{-13}	0.592	0.408
210	3.29×10^{-11}	7.28×10^{-13}	0.656	0.344	5.24×10^{-13}	0.601	0.399
220	3.30×10^{-11}	7.14×10^{-13}	0.699	0.301	5.11×10^{-13}	0.611	0.389
230	3.32×10^{-11}	7.16×10^{-13}	0.734	0.266	5.02×10^{-13}	0.621	0.379
240	3.33×10^{-11}	7.28×10^{-13}	0.762	0.238	4.98×10^{-13}	0.632	0.368
250	3.35×10^{-11}	7.48×10^{-13}	0.785	0.215	4.97×10^{-13}	0.642	0.358
260	3.37×10^{-11}	7.74×10^{-13}	0.803	0.197	5.00×10^{-13}	0.652	0.348

270	3.38×10^{-11}	8.06×10^{-13}	0.818	0.182	5.06×10^{-13}	0.663	0.337
280	3.40×10^{-11}	8.43×10^{-13}	0.831	0.169	5.14×10^{-13}	0.673	0.327
290	3.42×10^{-11}	8.84×10^{-13}	0.842	0.158	5.25×10^{-13}	0.683	0.317
300	3.43×10^{-11}	9.28×10^{-13}	0.850	0.150	5.38×10^{-13}	0.692	0.308
310	3.45×10^{-11}	9.77×10^{-13}	0.858	0.142	5.53×10^{-13}	0.702	0.298
320	3.47×10^{-11}	1.03×10^{-12}	0.864	0.136	5.70×10^{-13}	0.711	0.289
330	3.48×10^{-11}	1.08×10^{-12}	0.870	0.130	5.89×10^{-13}	0.719	0.281
340	3.49×10^{-11}	1.14×10^{-12}	0.875	0.125	6.10×10^{-13}	0.728	0.272
350	3.51×10^{-11}	1.20×10^{-12}	0.879	0.121	6.33×10^{-13}	0.735	0.265
360	3.52×10^{-11}	1.27×10^{-12}	0.882	0.118	6.58×10^{-13}	0.743	0.257
370	3.53×10^{-11}	1.34×10^{-12}	0.886	0.114	6.84×10^{-13}	0.750	0.250
380	3.54×10^{-11}	1.41×10^{-12}	0.888	0.112	7.12×10^{-13}	0.757	0.243
390	3.56×10^{-11}	1.48×10^{-12}	0.891	0.109	7.42×10^{-13}	0.763	0.237

145 Values in bold are the fitted values.

146

147

148

149

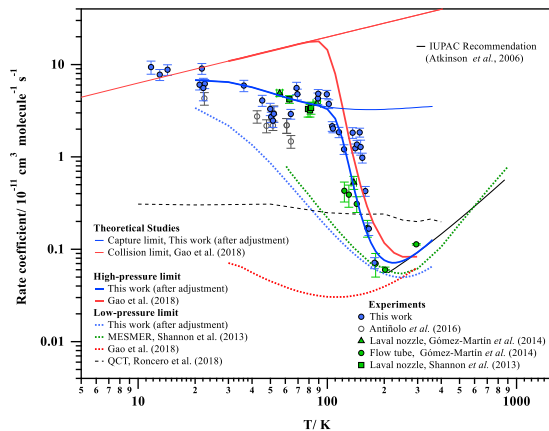
150

151

152

153

154

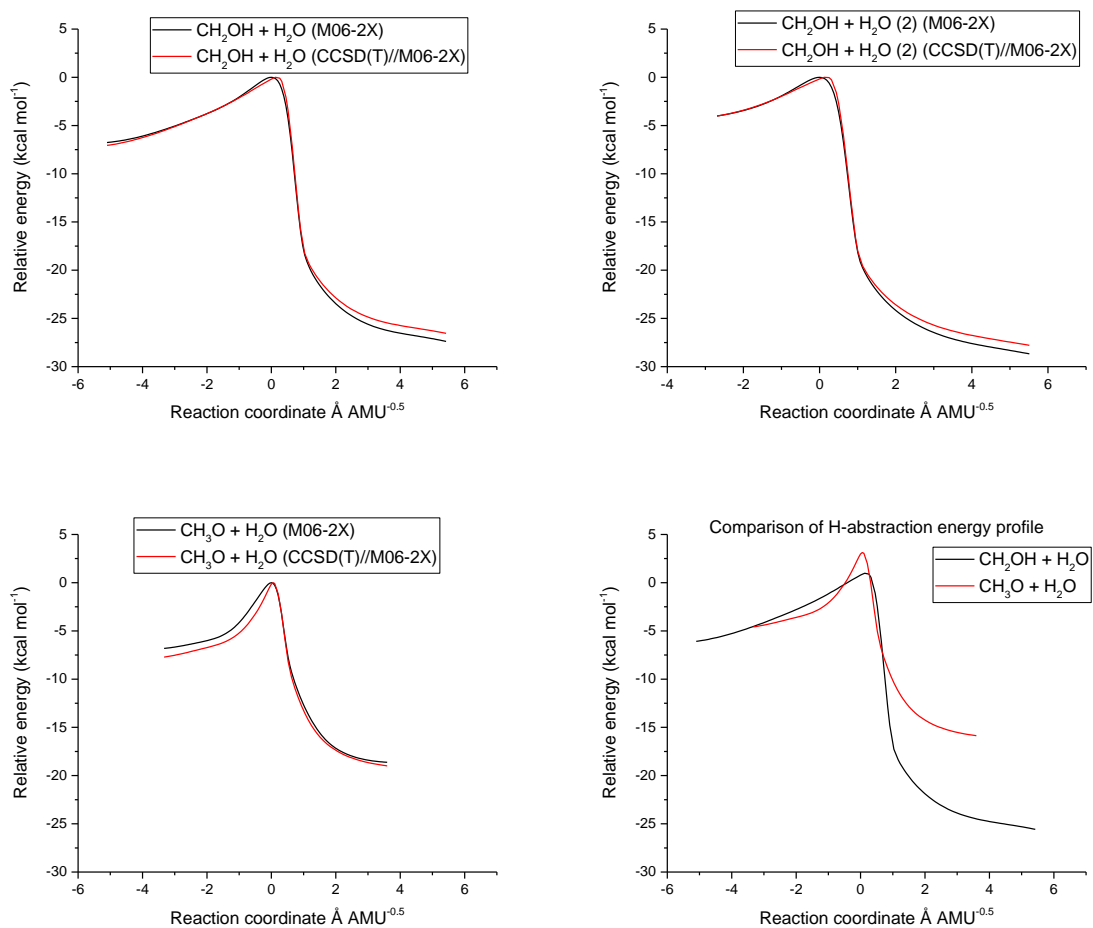


155

156

157 **Fig. S5** Theoretically predicted capture-, high-pressure, and low-pressure rate
 158 coefficients ($\text{cm}^3 \text{ molecule}^{-1} \text{ s}^{-1}$) for the $\text{CH}_3\text{OH} + \text{OH}$ reactions, after adjustment of the
 159 barrier heights for H-abstraction to match the IUPAC $k(300\text{K})$ and $Y(\text{CH}_3\text{O}+\text{H}_2\text{O})$
 160 recommendations, and scaling the low-energy $k(E)$ capture rate coefficient to the average of
 161 the experimental $k(20\text{K})$ values.

162



164 **Fig. S6** IRC energy profiles at the M06-2X/aug-cc-pVTZ and CCSD(T)//aug-cc-
 165 pVTZ//M06-2X levels of theory. Top left and right: 2 TS conformers for methyl-H
 166 abstraction. Bottom left: Lowest-energy TS conformer for hydroxy-H-abstraction. Bottom
 167 right: side-by-side comparison of the CCSD(T)//M06-2X energy profiles for the lowest-
 168 energy conformers of the two classes of H-abstraction.

169

170

171 Table S7 Relative energies (kcal mol⁻¹) for the critical points on the potential energy surface for the CH₃OH + OH reaction, at various
 172 selected levels of theory as available in this work and the literature. The values in bold are used in the kinetic analysis in this work.

Methodology	Reactants	Complex	TS _{b1}	TS _{b2}	Reference
M06-2X/aug-cc-pVQZ	0.00	-4.96	0.23	0.92	This work
CCSD(T)/aug-cc-pVQZ//M06-2X/aug-cc-pVQZ	0.00	-4.87	1.04	2.91	This work
IRCMax(CCSD(T)/aug-cc-pVTZ //M06-2X/ aug-cc-pVQZ)	0.00	-5.00	1.11	2.71	This work
CCSD(T)/CBS(DTQ)// IRCMax(CCSD(T)/aug-cc-pVTZ// M06-2X/ aug-cc-pVQZ)	0.00	-4.75	0.98	3.13	This work
B3LYP-D3/aug-cc-pVQZ	0.00		-2.55	-5.19	This work
IRCMax(CCSD(T)/aug-cc-pVTZ//B3LYP-D3/aug-cc-pVQZ)	0.00		2.77	3.38	This work
ωB97XD/aug-cc-pVQZ	0.00		-1.27	-1.01	This work
IRCMax(CCSD(T)/aug-cc-pVTZ//ωB97XD/aug-cc-pVQZ)	0.00		1.99	2.81	This work
CCSD(T)/6-311+G(3df,2p)//MP2/6-311+G(3df,2p)	0.00	-4.9	1.0	3.6	Xu and Lin ⁵
CCSD(T)-F12a/jun-cc-pVTZ//M08-HX/MG3S	0.00		1.46	3.06	Gao et al. ⁶
CCSD(T)/jun-cc-pVTZ//M08-HX/MG3S	0.00	-6.48			Gao et al. ⁶
CASPT2(11,11)/MG3S//M08-HX/MG3S	0.00			3.06	Gao et al. ⁶
CCSD(T)-F12a/cc-pVDZ-F12	0.00	-6.46	2.14	6.22	Roncero et al. ⁷
MRCI-F12+Q/cc-pVDZ-F12	0.00	-6.39	1.52	5.30	Roncero et al. ⁷
MPWB1K/6-31+G(d,p)	0.00	-5.64	0.14	1.17	Siebrand et al. ⁸

173

174 **Raw quantum chemical information**

```

175 *****
176 CH3OH + OH : M06-2X/aug-cc-pVQZ geometry
177 *****
178
179 CH3OH
180 -----
181 E(CCSD(T)/Aug-CC-pVDZ) (Hartree): -115.45498354
182 E(CCSD/Aug-CC-pVDZ) (Hartree): -115.44462500
183 T1 diagnostic: 0.010890
184 E(MP2/Aug-CC-pVDZ) (Hartree): -115.42130425
185 E(MP3/Aug-CC-pVDZ) (Hartree): -115.43932083
186 E(RHF/Aug-CC-pVDZ) (Hartree): -115.06185312
187 E(CCSD(T)/Aug-CC-pVTZ) (Hartree): -115.56223795
188 E(CCSD/Aug-CC-pVTZ) (Hartree): -115.54646879
189 T1 diagnostic: 0.009855
190 E(MP2/Aug-CC-pVTZ) (Hartree): -115.52891141
191 E(MP3/Aug-CC-pVTZ) (Hartree): -115.54321870
192 E(RHF/Aug-CC-pVTZ) (Hartree): -115.09250401
193 E(CCSD(T)/Aug-CC-pVQZ) (Hartree): -115.59312236
194 E(CCSD/Aug-CC-pVQZ) (Hartree): -115.57611768
195 T1 diagnostic: 0.009595
196 E(MP2/Aug-CC-pVQZ) (Hartree): -115.56306030
197 E(MP3/Aug-CC-pVQZ) (Hartree): -115.57360507
198 E(RHF/Aug-CC-pVQZ) (Hartree): -115.10002664
199 E(RM062X/Aug-CC-pVQZ) (Hartree): -115.72433910
200 Point group : CS
201 Electronic state : 1-A'
202 Cartesian coordinates (Angs):
203 C 0.046385 0.660592 -0.000000
204 O 0.046385 -0.751993 0.000000
205 H -0.438149 1.069902 0.888635
206 H 1.085396 0.977752 0.000000
207 H -0.438149 1.069902 -0.888635
208 H -0.858491 -1.065162 0.000000
209 Rotational constants (GHz): 129.3682900 25.0088300 24.1448400
210 Vibrational harmonic frequencies (cm-1):
211 294.3065 ( A'') 1070.1678 ( A') 1113.3611 ( A')
212 1184.7692 ( A'') 1370.3871 ( A') 1488.4511 ( A')
213 1511.0638 ( A'') 1520.8251 ( A') 3039.2214 ( A')
214 3091.6887 ( A'') 3150.9860 ( A') 3907.2995 ( A')
215 Zero-point correction (Hartree): 0.051811
216
217 OH
218 -----
219 E(CCSD(T)/Aug-CC-pVDZ) (Hartree): -75.58401208
220 E(CCSD/Aug-CC-pVDZ) (Hartree): -75.58065075
221 T1 diagnostic: 0.012115
222 E(MP2/Aug-CC-pVDZ) (Hartree): -75.56555498
223 E(MP3/Aug-CC-pVDZ) (Hartree): -75.57785261
224 E(PMP2/Aug-CC-pVDZ) (Hartree): -75.56731410
225 E(PMP3/Aug-CC-pVDZ) (Hartree): -75.57891269
226 E(PUHF/Aug-CC-pVDZ) (Hartree): -75.40654471
227 E(UHF/Aug-CC-pVDZ) (Hartree): -75.40362085
228 E(CCSD(T)/Aug-CC-pVTZ) (Hartree): -75.64558106
229 E(CCSD/Aug-CC-pVTZ) (Hartree): -75.63969742
230 T1 diagnostic: 0.010018
231 E(MP2/Aug-CC-pVTZ) (Hartree): -75.62633534
232 E(MP3/Aug-CC-pVTZ) (Hartree): -75.63790257
233 E(PMP2/Aug-CC-pVTZ) (Hartree): -75.62832327
234 E(PMP3/Aug-CC-pVTZ) (Hartree): -75.63904324
235 E(PUHF/Aug-CC-pVTZ) (Hartree): -75.42495141

```

```

236 E(UHF/Aug-CC-pVTZ) (Hartree): -75.42160059
237 E(CCSD(T)/Aug-CC-pVQZ) (Hartree): -75.66449481
238 E(CCSD/Aug-CC-pVQZ) (Hartree): -75.65801686
239 T1 diagnostic: 0.009499
240 E(MP2/Aug-CC-pVQZ) (Hartree): -75.64662073
241 E(MP3/Aug-CC-pVQZ) (Hartree): -75.65673028
242 E(PMP2/Aug-CC-pVQZ) (Hartree): -75.64863276
243 E(PMP3/Aug-CC-pVQZ) (Hartree): -75.65786986
244 E(PUHF/Aug-CC-pVQZ) (Hartree): -75.42997948
245 E(UHF/Aug-CC-pVQZ) (Hartree): -75.42659099
246 E(UM062X/Aug-CC-pVQZ) (Hartree): -75.73716255
247 Point group : C*v
248 Cartesian coordinates (Angs):
249 O 0.000000 0.000000 0.107876
250 H 0.000000 0.000000 -0.863009
251 Rotational constants (GHz): 0.0000000 565.5013271 565.5013271
252 Vibrational harmonic frequencies (cm-1):
253 3774.9088 ( SG)
254 Zero-point correction (Hartree): 0.008600
255
256 complex.CH3OH.OH
257 -----
258 E(CCSD(T)/Aug-CC-pVDZ) (Hartree): -191.04949837
259 E(CCSD/Aug-CC-pVDZ) (Hartree): -191.03525841
260 T1 diagnostic: 0.011561
261 E(MP2/Aug-CC-pVDZ) (Hartree): -190.99741315
262 E(MP3/Aug-CC-pVDZ) (Hartree): -191.02737930
263 E(PMP2/Aug-CC-pVDZ) (Hartree): -190.99913117
264 E(PMP3/Aug-CC-pVDZ) (Hartree): -191.02840916
265 E(PUHF/Aug-CC-pVDZ) (Hartree): -190.47587267
266 E(UHF/Aug-CC-pVDZ) (Hartree): -190.47298309
267 E(CCSD(T)/Aug-CC-pVTZ) (Hartree): -191.21842864
268 E(CCSD/Aug-CC-pVTZ) (Hartree): -191.19626132
269 T1 diagnostic: 0.010175
270 E(MP2/Aug-CC-pVTZ) (Hartree): -191.16590803
271 E(MP3/Aug-CC-pVTZ) (Hartree): -191.19151288
272 E(PMP2/Aug-CC-pVTZ) (Hartree): -191.16785052
273 E(PMP3/Aug-CC-pVTZ) (Hartree): -191.19262190
274 E(PUHF/Aug-CC-pVTZ) (Hartree): -190.52465603
275 E(UHF/Aug-CC-pVTZ) (Hartree): -190.52134495
276 E(CCSD(T)/Aug-CC-pVQZ) (Hartree): -191.26802431
277 E(CCSD/Aug-CC-pVQZ) (Hartree): -191.24402370
278 T1 diagnostic: 0.009785
279 E(MP2/Aug-CC-pVQZ) (Hartree): -191.22019895
280 E(MP3/Aug-CC-pVQZ) (Hartree): -191.24055607
281 E(PMP2/Aug-CC-pVQZ) (Hartree): -191.22216429
282 E(PMP3/Aug-CC-pVQZ) (Hartree): -191.24166384
283 E(PUHF/Aug-CC-pVQZ) (Hartree): -190.53713445
284 E(UHF/Aug-CC-pVQZ) (Hartree): -190.53378740
285 E(UM062X/Aug-CC-pVQZ) (Hartree): -191.47204925
286 Electronic state : 2-A
287 Cartesian coordinates (Angs):
288 C -1.376251 -0.497243 0.004285
289 O -0.542169 0.650622 -0.023596
290 H -2.098571 -0.483942 -0.811689
291 H -0.725213 -1.358128 -0.116930
292 H -1.902267 -0.586095 0.954668
293 H -1.064318 1.443143 0.104014
294 H 1.261635 0.246727 -0.001102
295 O 2.140449 -0.185402 0.004262
296 Rotational constants (GHz): 30.7119500 4.4599000 3.9937600
297 Vibrational harmonic frequencies (cm-1):
298 43.6350 52.9643 211.9748

```

```

299          290.6564          386.3313          607.9129
300          1079.4094          1099.4822          1187.0870
301          1367.0626          1490.5108          1511.0664
302          1521.4509          3056.7199          3119.2318
303          3161.7924          3614.5141          3910.7726
304 Zero-point correction (Hartree): 0.063134
305
306 TS.CH3OH+OH.CH2OH+H2O
307 -----
308 E (CCSD(T)/Aug-CC-pVDZ) (Hartree): -191.03690679
309 E (CCSD/Aug-CC-pVDZ) (Hartree): -191.02050998
310 T1 diagnostic: 0.023544
311 E (MP2/Aug-CC-pVDZ) (Hartree): -190.98071517
312 E (MP3/Aug-CC-pVDZ) (Hartree): -191.00880732
313 E (PMP2/Aug-CC-pVDZ) (Hartree): -190.98396957
314 E (PMP3/Aug-CC-pVDZ) (Hartree): -191.01088144
315 E (PUHF/Aug-CC-pVDZ) (Hartree): -190.44866616
316 E (UHF/Aug-CC-pVDZ) (Hartree): -190.44374969
317 E (CCSD(T)/Aug-CC-pVTZ) (Hartree): -191.20565197
318 E (CCSD/Aug-CC-pVTZ) (Hartree): -191.18092685
319 T1 diagnostic: 0.022051
320 E (MP2/Aug-CC-pVTZ) (Hartree): -191.14910322
321 E (MP3/Aug-CC-pVTZ) (Hartree): -191.17265663
322 E (PMP2/Aug-CC-pVTZ) (Hartree): -191.15257604
323 E (PMP3/Aug-CC-pVTZ) (Hartree): -191.17482499
324 E (PUHF/Aug-CC-pVTZ) (Hartree): -190.49695581
325 E (UHF/Aug-CC-pVTZ) (Hartree): -190.49168506
326 E (CCSD(T)/Aug-CC-pVQZ) (Hartree): -191.25552981
327 E (CCSD/Aug-CC-pVQZ) (Hartree): -191.22885767
328 T1 diagnostic: 0.021789
329 E (MP2/Aug-CC-pVQZ) (Hartree): -191.20361394
330 E (MP3/Aug-CC-pVQZ) (Hartree): -191.22187609
331 E (PMP2/Aug-CC-pVQZ) (Hartree): -191.20710905
332 E (PMP3/Aug-CC-pVQZ) (Hartree): -191.22404485
333 E (PUHF/Aug-CC-pVQZ) (Hartree): -190.50937492
334 E (UHF/Aug-CC-pVQZ) (Hartree): -190.50407135
335 E (UM062X/Aug-CC-pVQZ) (Hartree): -191.46043539
336 Electronic state : 2-A
337 Cartesian coordinates (Angs):
338 C -0.648965 0.676089 -0.004454
339 H -0.962787 1.249956 0.868940
340 O -1.238637 -0.584747 -0.083491
341 H -0.868492 1.215983 -0.920433
342 H 0.493504 0.587300 0.073495
343 H -1.126254 -1.039196 0.753625
344 O 1.836377 -0.080561 0.063668
345 H 1.575900 -0.748119 -0.590318
346 Rotational constants (GHz): 26.9959500 5.4928900 4.7961700
347 Vibrational harmonic frequencies (cm-1):
348 i760.7498 91.5443 149.1255
349 223.1943 404.1553 726.7028
350 1001.5301 1078.3864 1158.3796
351 1355.1687 1404.8678 1450.1849
352 1491.0536 1760.1556 3069.6643
353 3166.8582 3781.9194 3888.8959
354 Zero-point correction (Hartree): 0.059692
355
356 IRC information available
357 IRCMax information available
358 E (CCSD(T)/Aug-CC-pVDZ) (Hartree): -191.03668113
359 E (CCSD/Aug-CC-pVDZ) (Hartree): -191.01977365
360 T1 diagnostic: 0.025566
361 E (MP2/Aug-CC-pVDZ) (Hartree): -190.97969604

```

362 E(MP3/Aug-CC-pVDZ) (Hartree): -191.00705328
363 E(PMP2/Aug-CC-pVDZ) (Hartree): -190.98366238
364 E(PMP3/Aug-CC-pVDZ) (Hartree): -191.00955502
365 E(PUHF/Aug-CC-pVDZ) (Hartree): -190.44519131
366 E(UHF/Aug-CC-pVDZ) (Hartree): -190.43930455
367 E(CCSD(T)/Aug-CC-pVQZ) (Hartree): -191.25525482
368 E(CCSD/Aug-CC-pVQZ) (Hartree): -191.22792783
369 T1 diagnostic: 0.023882
370 E(MP2/Aug-CC-pVQZ) (Hartree): -191.20248982
371 E(MP3/Aug-CC-pVQZ) (Hartree): -191.21995523
372 E(PMP2/Aug-CC-pVQZ) (Hartree): -191.20669507
373 E(PMP3/Aug-CC-pVQZ) (Hartree): -191.22255444
374 E(PUHF/Aug-CC-pVQZ) (Hartree): -190.50573160
375 E(UHF/Aug-CC-pVQZ) (Hartree): -190.49947679
376 E(CCSD(T)/Aug-CC-pVTZ) (Hartree): -191.20535051
377 E(CCSD/Aug-CC-pVTZ) (Hartree): -191.17999466
378 T1 diagnostic: 0.024119
379 E(MP2/Aug-CC-pVTZ) (Hartree): -191.14797260
380 E(MP3/Aug-CC-pVTZ) (Hartree): -191.17073752
381 E(PMP2/Aug-CC-pVTZ) (Hartree): -191.15215430
382 E(PMP3/Aug-CC-pVTZ) (Hartree): -191.17333528
383 E(PUHF/Aug-CC-pVTZ) (Hartree): -190.49332545
384 E(UHF/Aug-CC-pVTZ) (Hartree): -190.48710401
385 Electronic state : 2-A
386 Cartesian coordinates (Angs):
387 C -0.643521 0.674339 -0.004799
388 H -0.937038 1.249408 0.874709
389 O -1.241984 -0.577712 -0.083652
390 H -0.851152 1.218255 -0.920942
391 H 0.527465 0.555807 0.069479
392 H -1.134023 -1.034256 0.753326
393 O 1.826768 -0.082630 0.064053
394 H 1.577601 -0.752518 -0.590993
395 Rotational constants (GHz): 27.2490730 5.5243405 4.8292264
396
397 TS.CH3OH+OH.CH2OH+H2O.b
398 -----
399 E(CCSD(T)/Aug-CC-pVDZ) (Hartree): -191.03563250
400 E(CCSD/Aug-CC-pVDZ) (Hartree): -191.01926707
401 T1 diagnostic: 0.023831
402 E(MP2/Aug-CC-pVDZ) (Hartree): -190.97934715
403 E(MP3/Aug-CC-pVDZ) (Hartree): -191.00754726
404 E(PMP2/Aug-CC-pVDZ) (Hartree): -190.98253854
405 E(PMP3/Aug-CC-pVDZ) (Hartree): -191.00959725
406 E(PUHF/Aug-CC-pVDZ) (Hartree): -190.44765444
407 E(UHF/Aug-CC-pVDZ) (Hartree): -190.44284334
408 E(CCSD(T)/Aug-CC-pVTZ) (Hartree): -191.20429305
409 E(CCSD/Aug-CC-pVTZ) (Hartree): -191.17961126
410 T1 diagnostic: 0.022317
411 E(MP2/Aug-CC-pVTZ) (Hartree): -191.14766193
412 E(MP3/Aug-CC-pVTZ) (Hartree): -191.17131880
413 E(PMP2/Aug-CC-pVTZ) (Hartree): -191.15107086
414 E(PMP3/Aug-CC-pVTZ) (Hartree): -191.17346215
415 E(PUHF/Aug-CC-pVTZ) (Hartree): -190.49598333
416 E(UHF/Aug-CC-pVTZ) (Hartree): -190.49081830
417 E(CCSD(T)/Aug-CC-pVQZ) (Hartree): -191.25414399
418 E(CCSD/Aug-CC-pVQZ) (Hartree): -191.22751788
419 T1 diagnostic: 0.022061
420 E(MP2/Aug-CC-pVQZ) (Hartree): -191.20214333
421 E(MP3/Aug-CC-pVQZ) (Hartree): -191.22050640
422 E(PMP2/Aug-CC-pVQZ) (Hartree): -191.20557459
423 E(PMP3/Aug-CC-pVQZ) (Hartree): -191.22264992
424 E(PUHF/Aug-CC-pVQZ) (Hartree): -190.50841627

```

425 E(UHF/Aug-CC-pVQZ) (Hartree): -190.50321820
426 E(UM062X/Aug-CC-pVQZ) (Hartree): -191.45910069
427 Electronic state : 2-A
428 Cartesian coordinates (Angs):
429 C 0.629622 0.656595 0.008737
430 H -0.470824 0.444801 -0.231862
431 H 1.000218 1.336005 -0.753678
432 H 0.656192 1.127463 0.993345
433 O 1.356348 -0.526056 -0.059557
434 H 0.982781 -1.160126 0.556348
435 O -1.819132 -0.240785 -0.075075
436 H -2.243832 0.447019 0.460483
437 Rotational constants (GHz): 28.8162800 5.2052500 4.5898400
438 Vibrational harmonic frequencies (cm-1):
439 1726.1472 57.1726 113.6145
440 220.0909 379.8244 687.5832
441 979.8316 1110.9096 1179.4995
442 1314.7005 1395.5790 1432.8677
443 1493.4200 1852.5499 3060.3046
444 3157.6019 3787.3519 3882.7353
445 Zero-point correction (Hartree): 0.059473
446
447 IRC information available
448 IRCMax information available
449 E(CCSD(T)/Aug-CC-pVDZ) (Hartree): -191.03543676
450 E(CCSD/Aug-CC-pVDZ) (Hartree): -191.01859617
451 T1 diagnostic: 0.025706
452 E(MP2/Aug-CC-pVDZ) (Hartree): -190.97839686
453 E(MP3/Aug-CC-pVDZ) (Hartree): -191.00593061
454 E(PMP2/Aug-CC-pVDZ) (Hartree): -190.98222225
455 E(PMP3/Aug-CC-pVDZ) (Hartree): -191.00836571
456 E(PUHF/Aug-CC-pVDZ) (Hartree): -190.44443183
457 E(UHF/Aug-CC-pVDZ) (Hartree): -190.43876210
458 E(CCSD(T)/Aug-CC-pVQZ) (Hartree): -191.25390416
459 E(CCSD/Aug-CC-pVQZ) (Hartree): -191.22666942
460 T1 diagnostic: 0.024012
461 E(MP2/Aug-CC-pVQZ) (Hartree): -191.20109667
462 E(MP3/Aug-CC-pVQZ) (Hartree): -191.21873672
463 E(PMP2/Aug-CC-pVQZ) (Hartree): -191.20515990
464 E(PMP3/Aug-CC-pVQZ) (Hartree): -191.22126767
465 E(PUHF/Aug-CC-pVQZ) (Hartree): -190.50504474
466 E(UHF/Aug-CC-pVQZ) (Hartree): -190.49900613
467 E(CCSD(T)/Aug-CC-pVTZ) (Hartree): -191.20402489
468 E(CCSD/Aug-CC-pVTZ) (Hartree): -191.17875734
469 T1 diagnostic: 0.024242
470 E(MP2/Aug-CC-pVTZ) (Hartree): -191.14660667
471 E(MP3/Aug-CC-pVTZ) (Hartree): -191.16954828
472 E(PMP2/Aug-CC-pVTZ) (Hartree): -191.15064652
473 E(PMP3/Aug-CC-pVTZ) (Hartree): -191.17207813
474 E(PUHF/Aug-CC-pVTZ) (Hartree): -190.49262468
475 E(UHF/Aug-CC-pVTZ) (Hartree): -190.48661944
476 Electronic state : 2-A
477 Cartesian coordinates (Angs):
478 C 0.625042 0.655083 0.008854
479 H -0.502220 0.415617 -0.213849
480 H 0.975298 1.334184 -0.763094
481 H 0.645759 1.127966 0.992464
482 O 1.357280 -0.519861 -0.060668
483 H 0.993899 -1.154598 0.561373
484 O -1.809900 -0.242008 -0.075446
485 H -2.242034 0.441283 0.458894
486 Rotational constants (GHz): 29.0670594 5.2360921 4.6211182
487

```



```

488 TS.CH3OH+OH.CH3O+H2O
489 -----
490 E(CCSD(T)/Aug-CC-pVDZ) (Hartree): -191.03211315
491 E(CCSD/Aug-CC-pVDZ) (Hartree): -191.01400598
492 T1 diagnostic: 0.034701
493 E(MP2/Aug-CC-pVDZ) (Hartree): -190.97367378
494 E(MP3/Aug-CC-pVDZ) (Hartree): -190.99915664
495 E(PMP2/Aug-CC-pVDZ) (Hartree): -190.97786609
496 E(PMP3/Aug-CC-pVDZ) (Hartree): -191.00166923
497 E(PUHF/Aug-CC-pVDZ) (Hartree): -190.43489454
498 E(UHF/Aug-CC-pVDZ) (Hartree): -190.42851875
499 E(CCSD(T)/Aug-CC-pVTZ) (Hartree): -191.20184417
500 E(CCSD/Aug-CC-pVTZ) (Hartree): -191.17503426
501 T1 diagnostic: 0.032928
502 E(MP2/Aug-CC-pVTZ) (Hartree): -191.14291335
503 E(MP3/Aug-CC-pVTZ) (Hartree): -191.16377572
504 E(PMP2/Aug-CC-pVTZ) (Hartree): -191.14729428
505 E(PMP3/Aug-CC-pVTZ) (Hartree): -191.16636513
506 E(PUHF/Aug-CC-pVTZ) (Hartree): -190.48371385
507 E(UHF/Aug-CC-pVTZ) (Hartree): -190.47703717
508 E(CCSD(T)/Aug-CC-pVQZ) (Hartree): -191.25136376
509 E(CCSD/Aug-CC-pVQZ) (Hartree): -191.22253676
510 T1 diagnostic: 0.032522
511 E(MP2/Aug-CC-pVQZ) (Hartree): -191.19712582
512 E(MP3/Aug-CC-pVQZ) (Hartree): -191.21264923
513 E(PMP2/Aug-CC-pVQZ) (Hartree): -191.20152788
514 E(PMP3/Aug-CC-pVQZ) (Hartree): -191.21523395
515 E(PUHF/Aug-CC-pVQZ) (Hartree): -190.49597310
516 E(UHF/Aug-CC-pVQZ) (Hartree): -190.48926674
517 E(UM062X/Aug-CC-pVQZ) (Hartree): -191.45815376
518 Electronic state : 2-A
519 Cartesian coordinates (Angs):
520 C 1.273712 0.382793 -0.020015
521 H 1.136011 0.982927 -0.920356
522 O 0.403910 -0.718823 0.002903
523 H 2.284408 -0.027776 -0.036014
524 H 1.158461 1.012782 0.861220
525 H -0.557107 -0.418610 0.341725
526 O -1.623376 0.250957 0.078254
527 H -1.908317 -0.103154 -0.775737
528 Rotational constants (GHz): 32.6567600 6.4318100 5.6632800
529 Vibrational harmonic frequencies (cm-1):
530 i1311.7676 125.2912 185.5549
531 225.7753 409.8703 785.5099
532 1082.5724 1135.2644 1174.2201
533 1303.3837 1457.1804 1472.0747
534 1512.4416 1696.2149 3042.8788
535 3108.5652 3126.1101 3820.1591
536 Zero-point correction (Hartree): 0.058465
537
538 IRC information available
539 IRCMax information available
540 E(CCSD(T)/Aug-CC-pVDZ) (Hartree): -191.03183336
541 E(CCSD/Aug-CC-pVDZ) (Hartree): -191.01339686
542 T1 diagnostic: 0.034647
543 E(MP2/Aug-CC-pVDZ) (Hartree): -190.97334925
544 E(MP3/Aug-CC-pVDZ) (Hartree): -190.99816720
545 E(PMP2/Aug-CC-pVDZ) (Hartree): -190.97858191
546 E(PMP3/Aug-CC-pVDZ) (Hartree): -191.00120067
547 E(PUHF/Aug-CC-pVDZ) (Hartree): -190.43270968
548 E(UHF/Aug-CC-pVDZ) (Hartree): -190.42485912
549 E(CCSD(T)/Aug-CC-pVQZ) (Hartree): -191.25109778
550 E(CCSD/Aug-CC-pVQZ) (Hartree): -191.22182646

```

```

551      T1 diagnostic: 0.032676
552 E(MP2/Aug-CC-pVQZ) (Hartree): -191.19670111
553 E(MP3/Aug-CC-pVQZ) (Hartree): -191.21149949
554 E(PMP2/Aug-CC-pVQZ) (Hartree): -191.20212635
555 E(PMP3/Aug-CC-pVQZ) (Hartree): -191.21459731
556 E(PUHF/Aug-CC-pVQZ) (Hartree): -190.49367594
557 E(UHF/Aug-CC-pVQZ) (Hartree): -190.48553532
558 E(CCSD(T)/Aug-CC-pVTZ) (Hartree): -191.20160889
559 E(CCSD/Aug-CC-pVTZ) (Hartree): -191.17437365
560      T1 diagnostic: 0.033052
561 E(MP2/Aug-CC-pVTZ) (Hartree): -191.14253708
562 E(MP3/Aug-CC-pVTZ) (Hartree): -191.16268719
563 E(PMP2/Aug-CC-pVTZ) (Hartree): -191.14793964
564 E(PMP3/Aug-CC-pVTZ) (Hartree): -191.16579006
565 E(PUHF/Aug-CC-pVTZ) (Hartree): -190.48144373
566 E(UHF/Aug-CC-pVTZ) (Hartree): -190.47333346
567 Electronic state : 2-A
568 Cartesian coordinates (Angs):
569      C      1.273864      -0.382078      0.020014
570      H      1.137456      -0.979995      0.922016
571      O      0.404125      0.718645      -0.004247
572      H      2.284370      0.030409      0.035660
573      H      1.159118      -1.013164      -0.860423
574      H      -0.578921      0.406645      -0.333671
575      O      -1.621365      -0.250514      -0.078085
576      H      -1.907290      0.103526      0.774988
577 Rotational constants (GHz):  32.7291721    6.4379865    5.6695878
578
579
580

```

